Supporting Information

Exploring Thermoelectric Properties of Oligo(phenylene-ethynylene) Derivatives

Hang Chen[†a], Sara Sangtarash[*†b,c], Guopeng Li[†a], Markus Gantenbein[d], Wenqiang Cao[a], Afaf Alqorashi[b], Junyang Liu[a], Chunquan Zhang[e], Yulong Zhang[e], Lijue Chen[a], Yaorong Chen[a], Gunnar Olsen[d], Hatef Sadeghi[c], Martin R. Bryce*[d], Colin J. Lambert*[b], Wenjing Hong*[a]

Affiliations:

a. State Key Laboratory of Physical Chemistry of Solid Surfaces, College of Chemistry and Chemical Engineering, *i*ChEM, Xiamen University, Xiamen, 361005, China.

b. Department of Physics, Lancaster University, LA1 4YB, Lancaster, UK.

c. School of Engineering, University of Warwick, Coventry CV4 7AL, UK.

d. Department of Chemistry, Durham University, DH1 3LE, Durham, UK.

e. Pen-Tung Sah Institute of Micro-Nano Science and Technology, Xiamen University, Xiamen, 361005, China.

*Email of corresponding authors:

s.sangtarash@lancaster.ac.uk;

m.r.bryce@durham.ac.uk;

c.lambert@lancaster.ac.uk;

whong@xmu.edu.cn.

†*These authors contributed equally to this work.*

Table of Contents

S1. Experimental technique

Preparation of STM tips and Au substrate

To prepare sharp STM tips, the electrochemical etching method was used.[1] First we prepared a mixed solution of concentrated hydrochloric solution (containing 37% HCl) and ethanol with a proportion of 1:1 v/v. Then we placed and immersed a gold ring with a 3/4 height below the solution surface. A gold wire of 0.25 mm diameter (99.99%, Jiaming, Beijing) was immersed in the solution at center of the gold ring. Then a DC voltage of 2.3 V was applied between the wire and the ring, and the wire was electrochemically etched until severed then the etching stopped. The etched gold tip was rinsed by isopropanol thoroughly and cleaned by N_2 gas before further usage.

To prepare the gold substrates, we deposited a 10 nm Cr film and a 200 nm film of Au on Si wafers using electron beam evaporation. Then the wafer was cut into 30 mm × 10 mm units and cleaned by piranha solution for further measurement.

Self-assembly of monolayers

The gold substrate was immersed in a 100 μM solution of the molecule in 1,2,4-trichlorobenzene (99.9%, Sigma Aldrich) for 24 h. Then the device surface with the assembled monolayer was rinsed by 1,2,4-trichlorobenzene and dried by N_2 gas.

Measurement of single-molecule conductance and thermal voltage.

Single-molecule conductance measurements were obtained at room temperature using the home-built scanning tunnelling microscope break junction technique (STM-BJ) which is shown in Figure S1. Soft-contact mode was chosen for STM-BJ experiments, a 100 mV DC bias was applied between the gold

substrate and the tip. The tip, controlled by the motor and piezoelectric actuator, was brought close enough to the gold surface. The tunneling current was measured by a lab-built logarithmic I-V converter with a sampling rate of 20 kHz. The tip withdrew from the sample until the increase of tunneling current achieves the given threshold value. Spontaneous formation of stable molecular junction between the tip and the substrate was observed.[2] A blank control experiment was performed using a clean gold substrate without any molecule assembled.

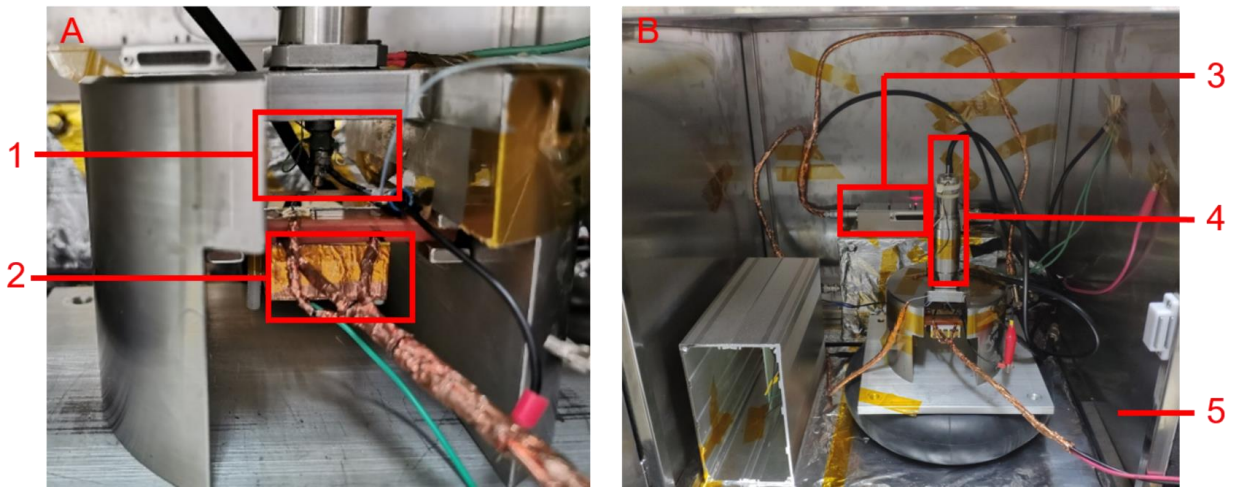

Figure S1. Photo of home-built STM-BJ machine. (A) Close up of the skeleton. (B) Overviews of the STM-BJ machine. 1 the STM tip, 2 Peltier device, 3 Voltage amplifier, 4 the motor, 5 the shield box.

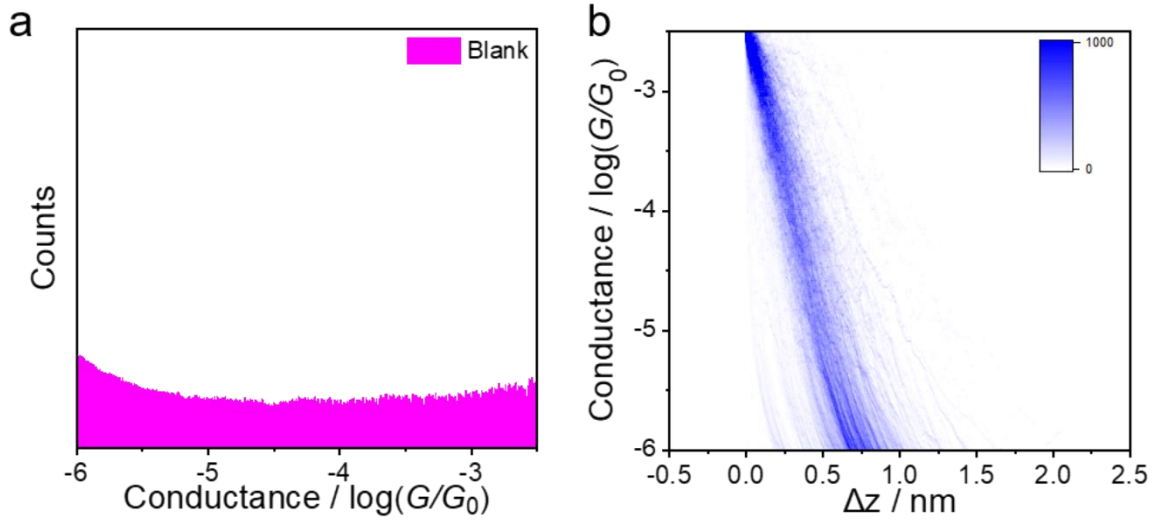

Figure S2. a) 1D conductance histogram constructed from 2000 conductance-distance traces without any selection for a clean gold substrate without any molecule assembled. b) 2D conductance histogram for a blank control experiment.

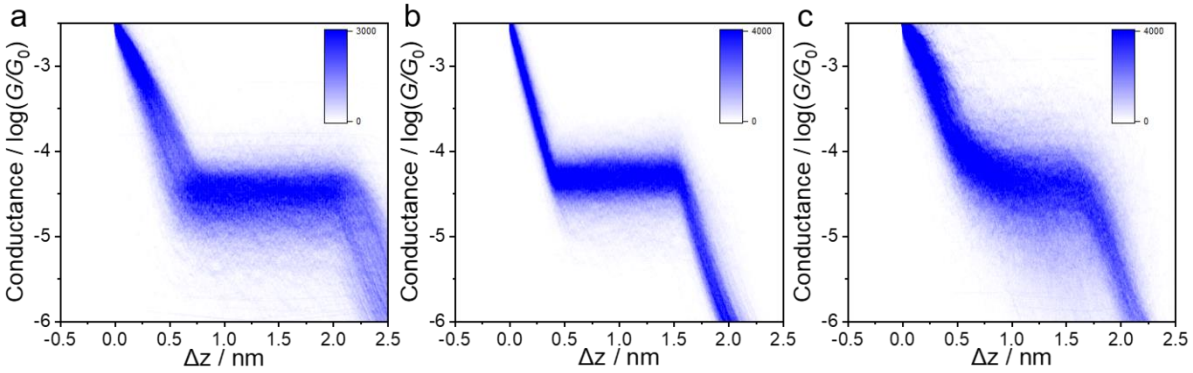

Figure S3. 2D conductance histograms for compounds **2**-**4** (a, b, c).

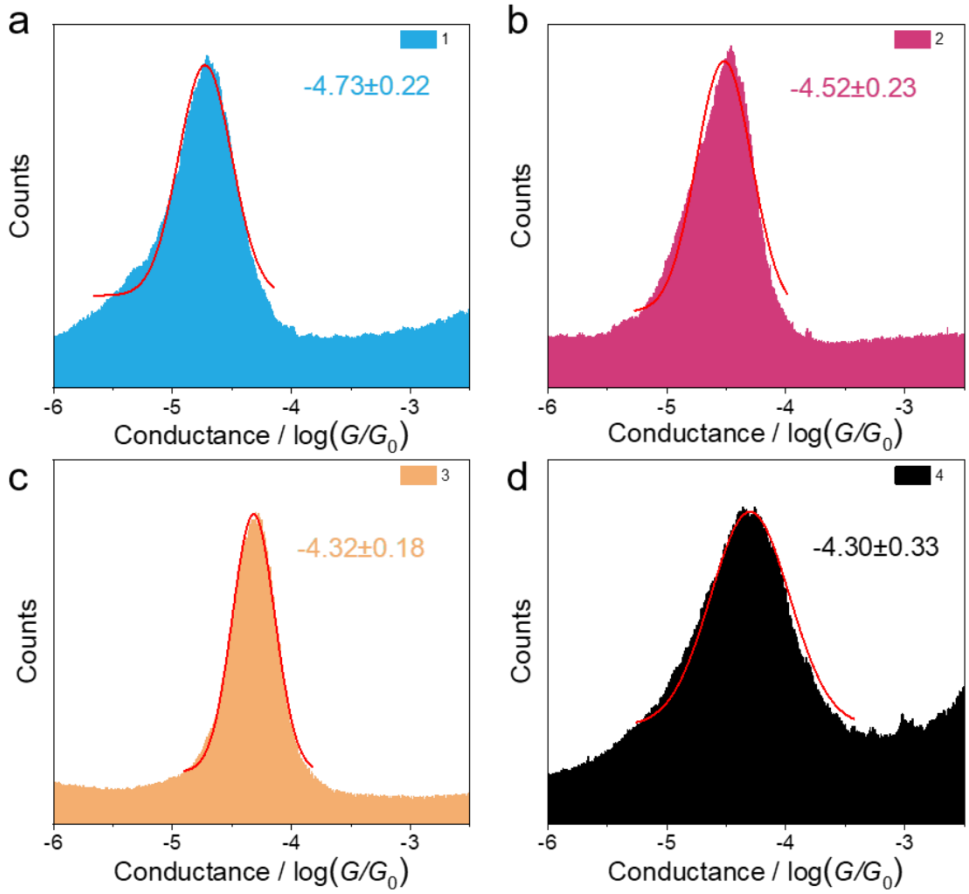

Figure S4. 1D conductance histograms constructed from 2000 conductance-distance traces without any selection for compounds **1**-**4** (a, b, c, d).

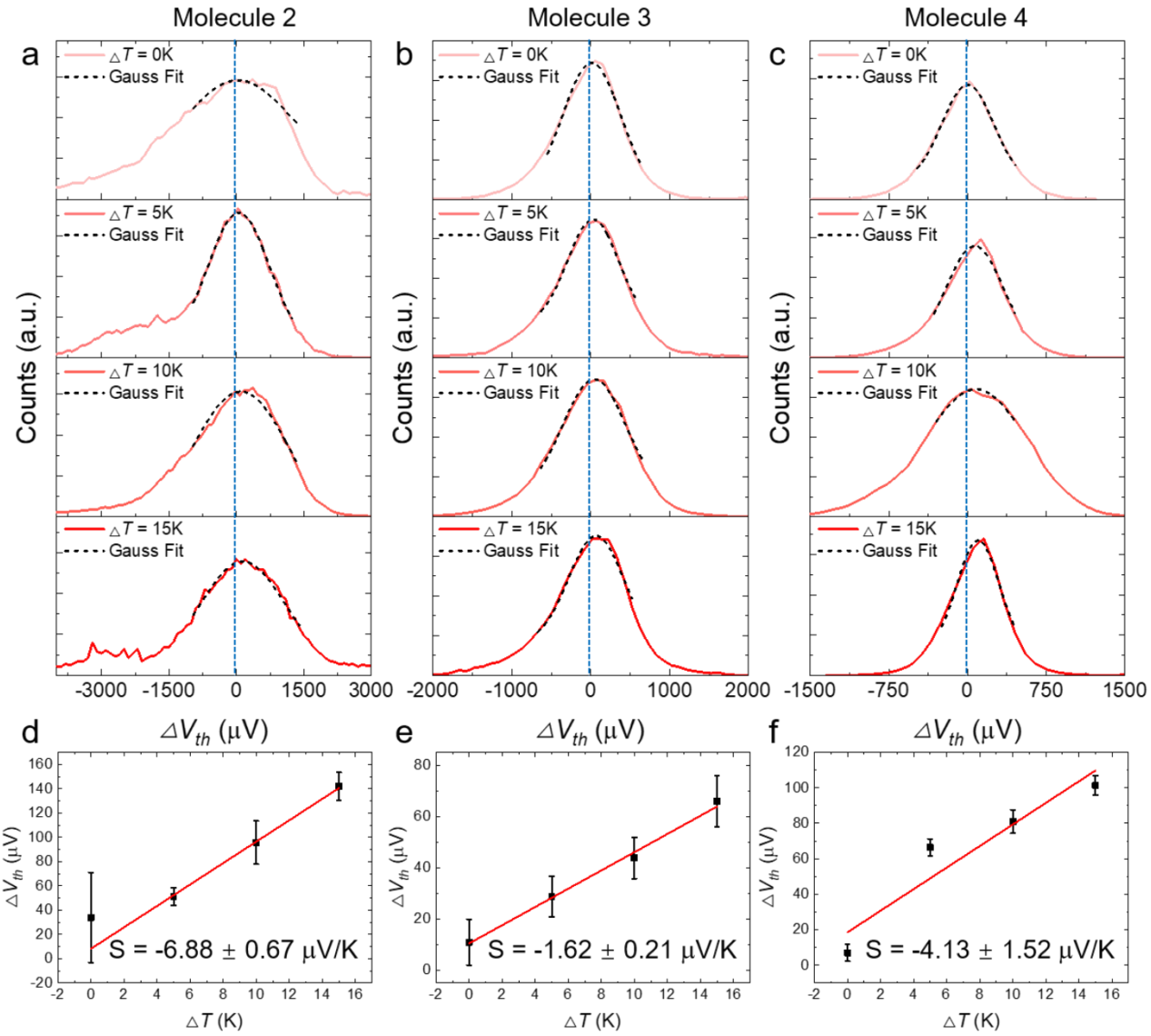

Figure S5. Results of thermopower measurements for compounds **2**-**4**, respectively. (a, b, c) Distribution of thermoelectric voltages at a series of ΔT as indicated. Gaussian fits plotted in black short dash line. Blue dash line indicates the Gaussian fitting centre of thermoelectric voltage at ΔT = 0 K. (d, e, f) The Seebeck coefficients obtained from the thermoelectric voltage as a function of ΔT. Red solid lines are the linear fitting curves.

To perform the thermoelectric measurement, an appropriate temperature difference should be formed between the tip and the substrate. A Peltier device was integrated under the substrate holder as a heater and the temperature was modulated by Proportion Integral Differential (PID) control. Single-molecule junctions were created following the same approach employed in the electrical conductance measurement. When the conductance plateau was monitored, the bias will firstly be switched from 0.1

V to 0.2 V. The tip was not hovered until the conductance under the 0.2 V bias was the same as that measured under 0.1 V bias. Once the tip was successfully hovered, the bias voltage will be switched to 0 V and the current amplifier will be cut off. Then the voltage amplifier is connected into the measuring circuit to start the thermoelectricity mode by a relay control. The thermal voltage is recorded by a differential-input voltage amplifier (de-dlpva-100-f, Femto) with 100 times amplification factor. After recording the thermal voltage data for a period of 100 ms (green area in Figure S6), the voltage amplifier will be cut off and the conductance mode will be switched back to 0.2 V again. If the measured conductance at this time is the same as before, we consider that all the thermovoltage data come from the single-molecule junctions. Finally, the bias will be switched back to 0.1 V, the tip will stop the hovering and be withdrawn from the sample until the tunneling conductance decreases to achieve the given threshold background. Thus, the measurement continues to repeat the above procedure for the next cycle.

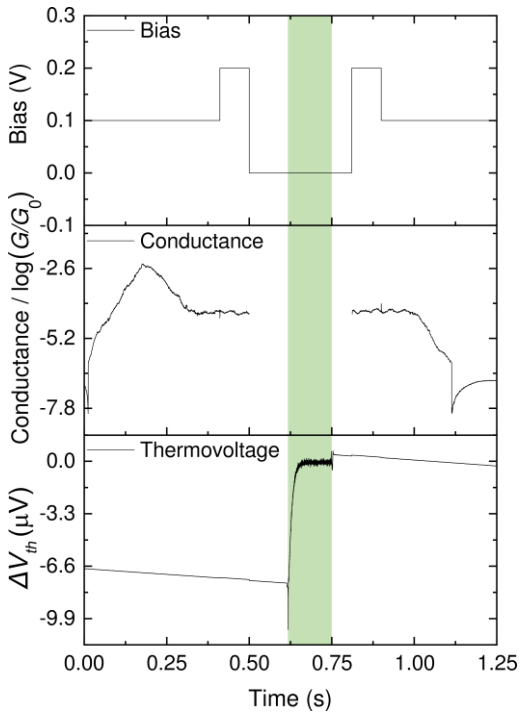

Figure S6. Typical data from thermoelectric measurements. From top to bottom: Bias voltage, measured conductance, thermovoltage of the molecule **1** as a function of time. The green area indicates the actual thermovoltage measurement period.

The relationship between measured voltage and the junction Seebeck coefficient[3, 4]

The relationship between thermoelectric voltage (V_{th}) and Seebeck coefficient (S) can be expressed as follow:

$$S = -\frac{V_{th}}{\Delta T} \quad (1)$$

$\Delta V_{th} = V_{hot} - V_{cold} = V_5 - V_6$, $\Delta T = T_{hot} - T_{cold} = T_3 - T_2$, V_n and T_n represent the electrical potential and temperature at node n (n=1-6) which is shown in Figure S6.

So the voltage difference to adjacent nodes in the circuit can be expressed as shown below:

$$V_2 - V_1 = -S_{Au}(T_2 - T_1) \quad (2)$$

$$V_3 - V_2 = -S_{junction}(T_3 - T_2) \quad (3)$$

$$V_4 - V_3 = -S_{Au}(T_4 - T_3) \quad (4)$$

$$V_5 - V_4 = -S_{Cu}(T_5 - T_4) \quad (5)$$

$$V_1 - V_6 = -S_{Cu}(T_1 - T_6) \quad (6)$$

Where $S_{junction}$, S_{Cu} and S_{Au} are the thermopower of the molecular junction, bulk metal Cu and Au, respectively. We assume that the whole system is thermal isolated. The tip is maintained at the ambient temperature $T_1 = T_2 = T_6 = T_5$ and the substrate was heated to a stable $T_3 = T_4$. So the equation can be simplified into

$$V_5 - V_6 = V_{th} = -S_{junction}(T_3 - T_2) - S_{Cu}(T_5 - T_4) \quad (7)$$

where $T_4 = T_3$ at the hot side and $T_5 = T_2$ at the ambient temperature (cold side).

So the final equation can be written as

$$S_{junction} = S_{Cu} - \frac{\Delta V_{th}}{\Delta T} \quad (8)$$

where S_{Cu} is a constant. When T = 300 K, S_{Cu} = 1.94 μV/K.[5]

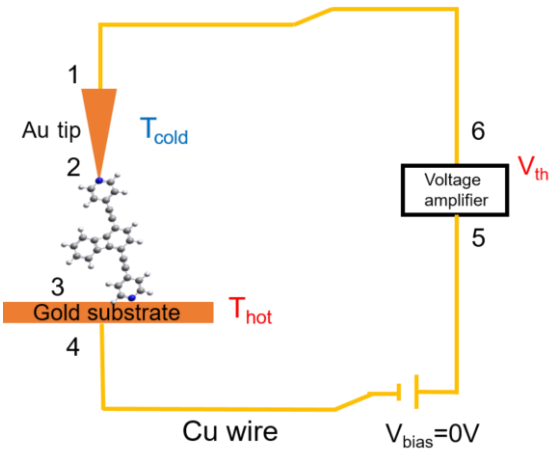

Figure S7. Schematic diagram of the thermoelectric voltage measurement circuit in the STM setup. Nodes 1-6 represent different nodes for the relevant temperature and electrical potentials.

S2. Theoretical calculations

Computational Methods

The optimized geometry and Hamiltonian of the device were obtained using the SIESTA[6] based on density functional theory (DFT). GGA-PBE exchange correlation functional is used. Double-ζ polarized (DZP) basis set is adopted for all atoms. The energy cut-off is defined with 250 Ry. The force for optimization is set as <10 meV/Å. The optimized geometry is shown in Figure S9 and used to obtain the transport properties in Figure 4. To investigate the effect of the molecular core, all calculations were carried out with the same electrode binding geometry. Calculations with different binding geometries of the molecules to the electrodes were presented in our previous work.[7] We have selected the junctions with the lowest energy and obtained good agreement with the measured conductance and the measured Seebeck coefficient. From past experience and also the paper,[8] the Seebeck coefficient is sensitive to the electrode configuration. In practice, this means that the Fermi energy would need to be adjusted to achieve an agreement with the experiment. By using the Hamiltonian obtained from SIESTA as input parameter, we calculate the transmission coefficient for electrons passing from the source to drain by using the Gollum quantum transport code[9] via the relation $T(E) = Trace(\Gamma_R(E)G^R(E)\Gamma_L(E)G^{R\dagger}(E))$, where, $\Gamma_{L,R}(E) = i\left(\sum_{L,R}(E) - \sum_{L,R}{}^{\dagger}(E)\right)$ describe the level broadening due to the coupling between

electrodes and the central scattering region, $\sum_{L,R}(E)$ are the retarded self-energies and $G^R = (ES - H - \sum_L - \sum_R)^{-1}$ is the retarded Green's function. The conductance could be calculated by the Landauer formula ($G = G_0 \int \mathrm{d}E\ \mathrm{T}(E)(-\partial \mathrm{f}/\partial E)$), where $G_0 = 2e^2/h$ is the conductance quantum, $f(E) = (1 + exp((E - E_F)/k_BT))^{-1}$ is the Fermi-Dirac distribution function, T is the temperature and k_B = 8.6×10^{-5} eV/K is the Boltzmann's constant. The Seebeck coefficient is given by: $\mathrm{S(T)} \approx -\alpha e \mathrm{T}(\frac{dlnT(E)}{dE})$, where $\alpha = \left(\frac{k_B}{e}\right)\frac{\pi^2}{3}$ is the Lorentz number.

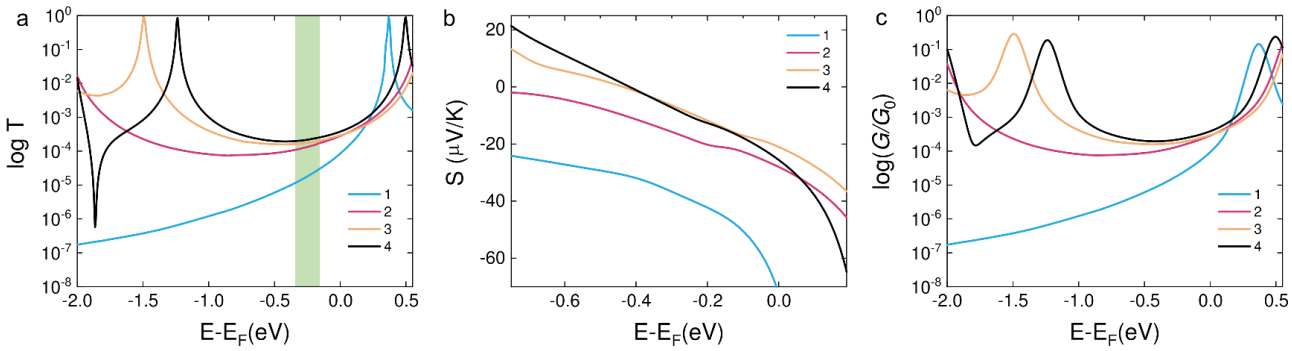

Figure S8: a) DFT results of the transmission coefficients with corrected gap (see methods section) for compounds **1-4**. (b) Seebeck coefficient of corresponding molecules. The highlighted area shows the Fermi energy at which the calculated transmission and the Seebeck coefficient are in qualitative agreement with the experimental findings. c) Electrical conductance of molecules **1-4**.

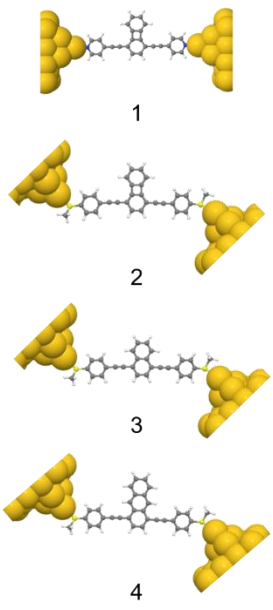

Figure S9: Relaxed structures of molecules **1-4**.

References

1. B. Ren, G. Picardi and B. Pettinger, *Rev. Sci. Instrum.*, 2004, **75**, 837-841.
2. W. Haiss, H. van Zalinge, S. J. Higgins, D. Bethell, H. Höbenreich, D. J. Schiffrin and R. J. Nichols, *J. Am. Chem. Soc.*, 2003, **125**, 15294-15295.
3. R. Miao, H. Xu, M. Skripnik, L. Cui, K. Wang, K. G. L. Pedersen, M. Leijnse, F. Pauly, K. Warnmark, E. Meyhofer, P. Reddy and H. Linke, *Nano Lett.*, 2018, **18**, 5666-5672.
4. P. Reddy, S.-Y. Jang, R. A. Segalman and A. Majumdar, *Science*, 2007, **315**, 1568-1571.
5. F. J. Blatt, *Thermoelectric Power of Metals*, Plenum Press, New York, 1976.
6. J. M. Soler, E. Artacho, J. D. Gale, A. García, J. Junquera, P. Ordejón and D. Sánchez-Portal, *J. Phys.: Condens. Matter*, 2002, **14**, 2745-2779.
7. M. Gantenbein, X. Li, S. Sangtarash, J. Bai, G. Olsen, A. Alqorashi, W. Hong, C. J. Lambert and M. R. Bryce, *Nanoscale*, 2019, **11**, 20659-20666.
8. R.-N. Wang, G.-Y. Dong, S.-F. Wang, G.-S. Fu and J.-L. Wang, *Phys. Chem. Chem. Phys.*, 2016, **18**, 28117-28124.
9. J. Ferrer, C. J. Lambert, V. M. García-Suárez, D. Z. Manrique, D. Visontai, L. Oroszlany, R. Rodríguez-Ferradás, I. Grace, S. W. D. Bailey, K. Gillemot, H. Sadeghi and L. A. Algharagholy, *New J. Phys.*, 2014, **16**, 093029.